QUALITY ANALYSIS FOR POSITIONING USING REALISTIC IMAGE-BASED 3D MAPS

Wenyang Liu, Ruiyuan Li, Jinling Wang, Xun Li
School of Surveying and Spatial Information Systems, University of New South Wales,
Sydney, NSW 2052, Australia;Tel:+61-2-93854184,Email:wenyang.liu@student.unsw.edu.au

KEY WORDS:Quality Analysis; Measurable image-based maps; 3D map

ABSTRACT:3D mapping has been used in multi-discipline applications. The traditional 3D mapping method needs specially trained people and expensive equipment to collect data and process data. Over recent years, as the rapid development of sensor technologies, computer vision and photogrammetry, the vision-based method to detailing works was brought to fill the gap and improve the efficiency of 3D mapping. The measureable realistic image-based (MRI) 3D maps can be employed with affordable cost and acceptable quality for industrial activities and business. In this paper, the quality analysis of point positioning with the MRI maps using least squares estimation is described. This paper also presents some initial results of point position measuring experiments conducted to test the quality of such an approach.

1. INTRODUCTION

The technology of computer vision, photogrammetry and sensors like cameras and Inertial Measurement Unit (IMU) are introduced to map the streets, mined field or undergroundareas as a new trend of 3D mapping. The next generation of map services will provide much more relevant information of what people want and context of an interested place. It bridges between “geographic location” and “cultural location”. It means maps are not only illustrating geometric coordinates, also representing the world vividly and transformation of meaningful knowledge into positioning such as the demonstration of the Google Street View. However, such vivid 3D maps only provide virtual experience in terms of photos, while a number of details representing the topographic and terrain attributes are all omitted, such as shapes and heights. To take measurements on objects within the geo-referenced images is valuable for both scientific and commercial applications.

In this paper, we propose a concept of spatial measurements with the measurable realistic image-based (MRI) maps.These new 3D maps arebased on geo-referenced realistic images, named as thegeo-referenced Street View, which are then used to implement of spatialmeasurementsVariousapplications can be implemented, such as measurement of object coordinates, distance measurement, objects’ orientation and elevation, measurement of areas or volume for a given section of the scene in the map, and reconstruction of 3D models. This paper mainly focuses on the quality analysis of the measurements of object coordinatesfor selected features in the images. The procedure of space intersection was conducted based on an assumption of known exteriorparameters of the geo-referenced images. Least squares estimation is taken to deal with redundancy of the overlapped images. TheDilution of Precision (DOP) values are introduced to evaluate the geometry quality of object coordinates. The reliability measures to evaluate how much impact of the outliers onobject coordinates ofobservation.

The paper is organized as follows. In the next section, the methodology is described. Section 3 will illustrate the initial numerical experimental results and which will be followed by the concluding remarks.

2. THE METHODOLOGYOF MRI MAPPING SYSTEMAND QUALITY CONTROL

2.1 The Measurable Realistic Image-basedMaps

MRI 3D mapping system includes three essential procedures: data collection, data processing and user-orientated

part, as shown in Figure1. For data acquisition, stereo cameras, GPS and IMU sensors could be used, e,g., in aloosely coupledmodel on a mobile platform. Stereo image matching in particular is of fundamental importance toin photogrammetry, which is widely applied in practices, such as navigation, guidance, automatic surveillance, robot vision, and the mapping sciences (Gruen, 1985). The all sensors constantly obtain synchronized data for the determination of 3D coordinates and the attitude parameters of a moving platform. In the step of data processing, each digital image will be associated with such parameters, called 6 Degrees of Freedom (6DoF), and then are stored in a database. The user terminal enables a user to obtain spatial measurementsas defined above, such as positioning, distance measurements between features, from the MRI 3D maps.

For the function of object coordinates measurement,user should clicka point or featureon the MRI 3D maps and this selected point/feature will be matched with a corresponding point onthe neighboring overlapping images in the database to obtain objective coordinates. Generally, SIFT (Scale-invariant feature transform) is most popular for feature-based image matching that is a robust algorithm to deal with the image noise effects. The SIFT finding candidate matching features based on Euclidean distance of their feature vectors and using SIFT feature for matching (Lowe, 2004). However, there is a probability that usermight have clickeda point which is not a SIFT feature point, and thus, the SIFT matching may be failed in the user terminal. Therefore, manual selection of a corresponding point instead using the SIFT procedure is applied at this development stage for our approach.

The quality of spatial measurements is mainly basedon three main aspects. The first factor that should be considered is the geometric distortion errors of a vision sensor. The vision calibration could be conducted before or after data collection. On the other hand, the precision of measurements of the image coordinates for a selected object point on the overlapped images could also affect the accuracy of 3D measurements.One interested point can be matched on several overlapping images. The last one is related to the object coordinate estimation which essentially refers to the geometry of the mathematical model of the stereo images.The highly accurate point positioning measurement can be achieved if the suitable configurations of the camera position, object size and the accuracy of the elements of 6Degree of Freedomfor each image (Luhmann, 2009).

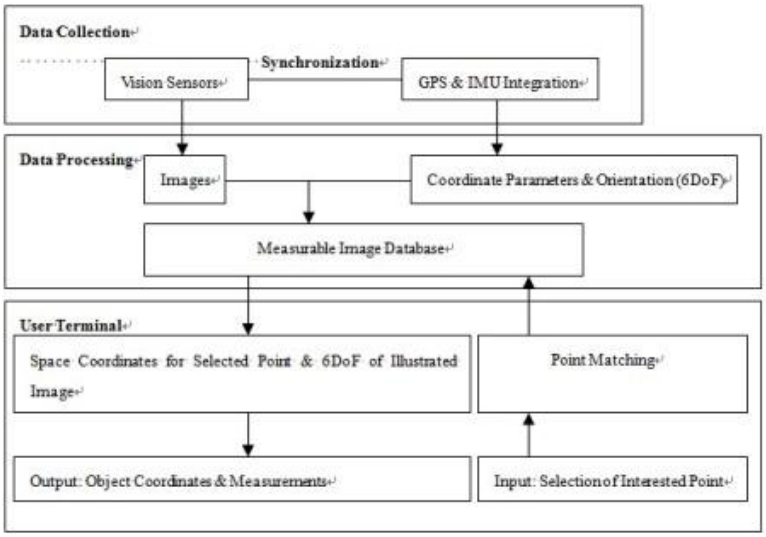

Figure 1. The Flow Chart of MRI 3D Mapping System

2.2 The Quality Control of Object Coordinate Determination

In our previous work, we investigated the accuracy of object coordinates and geometry measurement of each geo-referenced image. In this paper, our work mainly focuses on the quality analysis of the measurement of

Objectcoordinates.In order to determine object coordinates based on the overlapping images and their known 6 DoF parameters., theprocedure of space intersection was conducted.Object coordinates can be solved with minimum two geo-referenced images based on the well-known collinearity equations.

In our approach more than two geo-referenced images have been applied to ensure a good accuracy of object coordinates, so least squares estimation is taken to deal with redundant geo-referenced overlapping imagesThe geometric transformation implies the use of the centre perspective algorithm, which can be supplemented by some corrections for the deterministic errors (Makarovic, 1995). The strategy of quality analysis is based on least squares estimation, the function and stochastic model are illustrated as below:

$$\mathbf{v} = \mathbf{A}\hat{\mathbf{x}} - \mathbf{l} \tag{1}$$

$$\mathbf{D} = \boldsymbol{\sigma}_0^2\mathbf{Q} = \boldsymbol{\sigma}_0^2\boldsymbol{P}^{-1} \tag{2}$$

$$\hat{\boldsymbol{\sigma}}_0 = \sqrt{\frac{\mathbf{v}^T\mathbf{P}\mathbf{v}}{\mathbf{n}-\mathbf{u}}} \tag{3}$$

where Equation (1) is the function model and Equation (2) denotes the stochastic model. In this paper, the image observation model is based on the collinearity equations:

$$\begin{cases} \mathbf{x} = -\mathbf{f}\dfrac{\mathbf{a_1}(\mathbf{X}-\mathbf{X_S})+\mathbf{b_1}(\mathbf{Y}-\mathbf{Y_S})+\mathbf{c_1}(\mathbf{Z}-\mathbf{Z_S})}{\mathbf{a_3}(\mathbf{X}-\mathbf{X_S})+\mathbf{b_3}(\mathbf{Y}-\mathbf{Y_S})+\mathbf{c_3}(\mathbf{Z}-\mathbf{Z_S})} \\ \mathbf{y} = -\mathbf{f}\dfrac{\mathbf{a_2}(\mathbf{X}-\mathbf{X_S})+\mathbf{b_2}(\mathbf{Y}-\mathbf{Y_S})+\mathbf{c_2}(\mathbf{Z}-\mathbf{Z_S})}{\mathbf{a_3}(\mathbf{X}-\mathbf{X_S})+\mathbf{b_3}(\mathbf{Y}-\mathbf{Y_S})+\mathbf{c_3}(\mathbf{Z}-\mathbf{Z_S})} \end{cases} \tag{4}$$

which describes the relationship between the focus, image point and corresponding object point (They are on the same line of light). *x* and *y* on the left hand side are the measured coordinates for the image point within the image frame. ***f*** is the focal length of camera. *X, Y* and *Z* on the right hand side are the object coordinates for that point. At the mean time, Xs, Ys and Zs are the coordinates of a camera in the object frame. Moreover, a_1, a_2, a_3, b_1, b_2, b_3, c_1, c_2 and c_3 are the elements from the rotation matrix from the spatial image coordinate frame to the object frame which are derived from the exterior parameters Omega, Phi and Kappa. In this case, collinearity equations linearization will be done by taking the partial derivativewith regard to the object coordinates X, Y and Z to be determined. :

$$\mathbf{A} = \begin{bmatrix} \frac{\partial \mathbf{x}}{\partial \mathbf{X}} & \frac{\partial \mathbf{x}}{\partial \mathbf{Y}} & \frac{\partial \mathbf{x}}{\partial \mathbf{Z}} \\ \frac{\partial \mathbf{y}}{\partial \mathbf{X}} & \frac{\partial \mathbf{y}}{\partial \mathbf{Y}} & \frac{\partial \mathbf{y}}{\partial \mathbf{Z}} \end{bmatrix} \tag{5}$$

$$\hat{\mathbf{x}} = [\mathbf{dX_{oc}} \quad \mathbf{dY_{oc}} \quad \mathbf{dZ_{oc}}]^T \tag{6}$$

$$\mathbf{l} = [\mathbf{x} - (\mathbf{x})] \tag{7}$$

Where the elements of x, (x)…denote the observed value of image coordinates and the initial values of image coordinate, respectively. $\mathbf{X_{oc}}, \mathbf{Y_{oc}}, \mathbf{Z_{oc}}$are the corrections to the approximate coordinates of a selected object.

The Dilution of Precision (DOP) valueswere introduced that they were defined to evaluate the impact of geometry changes on the objective coordinates. The values were obtained by least squares estimation as:

$$\mathrm{XDOP} = \mathrm{G_x} \quad \mathrm{YDOP} = \mathrm{G_y} \quad \mathrm{ZDOP} = \mathrm{G_z} \tag{12}$$

$$\mathrm{PDOP} = \sqrt{\mathrm{G_x^2} + \mathrm{G_y^2} + \mathrm{G_z^2}} \tag{13}$$

The elements of$\mathrm{G_x}$, $\mathrm{G_\omega}$ … are derived from the diagonal elements of the matrix $(\mathrm{A^TA})^{-1}$, where A is the design

matrix of the least squares. The PDOP represents the position DOP.

2.3 RELIABILITY AND OUTLIER DETECTION

Outliers within any photogrammetric experiments could come from gross errorsin the image coordinates. The statistical processing with the so-called Global Test and data snooping methods are normally made to deal with outliers. The more information of mathematics on these methods can be found in (Kavouras,, 1982; Teunissen; 1990; Wang & Chen , 1994). The former processing is used to indicate whether observations contain any gross errors. The posteriori variance $\hat{\sigma}_0$ and the priori variance σ_0 are applied, giventhe confidence level (1-α) with the hypothesis $H_0: \hat{\sigma}_0^2 = \sigma_0^2$ under $H_a: \hat{\sigma}_0^2 > \sigma_0^2$while assuming the statistic $\hat{\sigma}_0/\sigma_0$ following the $F_{r,\infty}$distribution, then if the ratio over the F (f,∞; 1-α) in one tail test, the global test would be failed, whichindicates that there are outliers in observations. The data snooping is applied to check which observation probably contains gross errors. The mean shift of observation‘sexpectation can be expressed with outliers, the test statistic is showed as below:

$$W_i = \frac{\widehat{\nabla S_i}}{\sqrt{D_{\nabla S_i}}} \tag{14}$$

where $\widehat{\nabla S_i}$is the estimated outlier in the *i*th observation, D∇Si denotes its variance, $W_i$would follow the normal distribution *N (0, 1)*in the situation of non-outlier existing, otherwise the two tails test is conducted with the confidence level ($1-\alpha_0$) as:

$$\text{If} \qquad |W_i| > N\left(0{,}1; 1 - \frac{\alpha 0}{2}\right) \tag{15}$$

Then outlier exist, the outlier is determined by the largest value of $|W_i|$. Then the observation which is associated with the largest W value iscancelled and the procedures of global test and data snooping arerepeated till alloutliersare cancelled. With the statistic defined by the equation (14), the inverse operation should define the reliability measure as expressed in equation (16), and then with a diagonal weight matrix *P* it simplified to equation (17):

$$\nabla_0 S_i = \frac{\sigma_0\, \delta_0}{\sqrt{e_i^T P Q_v P e_i}} \tag{16}$$

$$\nabla_0 S_i = \frac{\delta_0}{\sqrt{r_i}} \sigma_{l_i} \tag{17}$$

in which$\nabla_0 S_i$ is known as the minimal detectable bias (MDB) in the *i*th observation, $Q_v$cofactor matrix of residuals and $e_i$equal to 1,δ_0 denotes the lower bound value for non-central parameter,$r_i$refers to the redundancy number.

3. EXPERIMENTS

The aim of the experiments is to explore the relationship between amount of overlapping images and the quality of positioning. They were conducted in the indoor environment with a calibrated Canon EOS450D camera with a resolution of 4272*2848 square pixels. For the photogrammetric frame which was applied to the calculation, the y axis points the opposite direction to be a right-handed frame. The six images have different angles towards the object wall with an approximate range of 6 to 10 meters (Figure 3). As only space intersection of photogrammetry was investigated here, all the images are supposed to have the known parameters of 6DoF which were calculated by space resection with scattered control points 1, 3, 7, 8, 9, 10, 17, 18 in Figure 2. In our previous work, all control points were also used as tie points, but in this paper the control points were not be used as tie points. 18 points were measured by a total station and treated as the ground truth. The object coordinate frame is a right hand frame in that y axis pointing was toward to the wall containing the objects, x axis paralleled with it, and z axis was perpendicular to the x-y plane towards up.

3.1 Analysis of DOP Values

This test was conducted with2, 3, 4, 5 and 6images respectively. In each experiment just one tie point was used for DOPs evaluation. Here taking Points 6 and 15 as the examples with different amount of geo-referenced-images. The former point is close to the central of the image and the later one is near the edge of the image. As Figure 4a and 4b show that the PDOP and YDOP for Points 6 and 15 dropped remarkably from 2 images to 4 images. The reason is that much more redundancy exists in the 4 images situation which allows the least squares adjustment for results. Although there is still a trend to improve geometry of the tie points with more images the accuracy improvements become insignificant beyond 4, 5 and 6 overlapped images. The factor dominating the phenomenon is whether the observations have significant geometrical strength to further enhance the adjustment. The XDOPs and ZDOPs were extremely close all the time. Obviously, the DOP value of depth (Y axis) was always the worst geometry among all the axes. Comparing the DOPs results of Points 6 and 15, DOP values of Point 6 was slightly better than that of Point 15 The experiment revealed that implementation of good geometry for the interested points is probably required with at least four overlapped images for observing. The selection of the measured point should be close to the centre of the images involved

3.2 Testing for Reliability and Outlier Detection

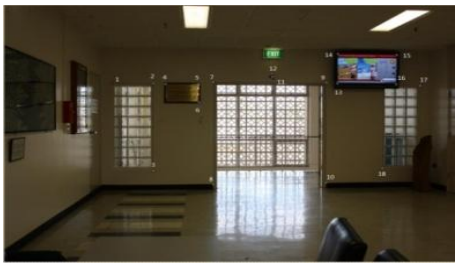

Figure 2. Experiments Illustration

Figure 3. Images Taken for Experiments

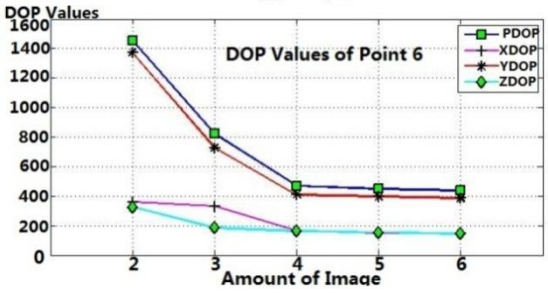

Figure 4a.DOP Values for Point 6

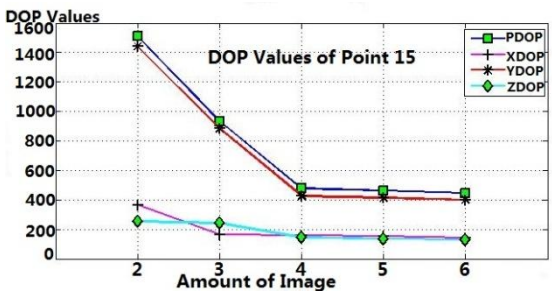

Figure 4b. DOP Values for Point 15

The test conducted with 3 and 4observing images was based on Point 2.The observation noise level was set to be 0.000015 m. For the global test, the confidence level was set to be 0.05. In data snooping the confidence level was set to 0.001.Fig 5and Fig 7 illustrated the minimum detectable bias (MDB) of x, y image coordinate respectively. Fig 6 and Fig 8 showed the results of data snooping for Point 2 with three images. Each image included a pair of x, y observation. The results show no outliner contained in both x and y image coordinates. The object coordinates of Point 2 were -3.386 m (X), 5.099 m (Y) and 2.087 m (Z) respectively. Comparing with the ground truth which are -3.396 m, 6.015 m and 2.076 m, the measured position had the differences of 10mm, -16 mm and 9 mm on X, Y and Z, respectively. Then, the fourth image was added into the experiment. Fig 9 and Fig 11 are the minimum detectable bias (MDB) of x, y image coordinates. Fig 10and Fig 12 showed the results of data snooping for Point 2 with four images. The figures illustrated the newly added image contained outliers for the x, y observation of Point 2 in the image frame, while the measured position of Point 2 was even worse than the situation of three images. The measured position was -3.420 m, 6.153 m, 2.094 m. Comparing to the ground truth, there were deviations of -24

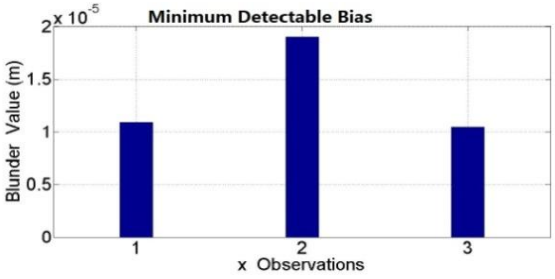

Figure 5.Minimum Detectable Bias of x Image Coordinate (Point 2 with three images)

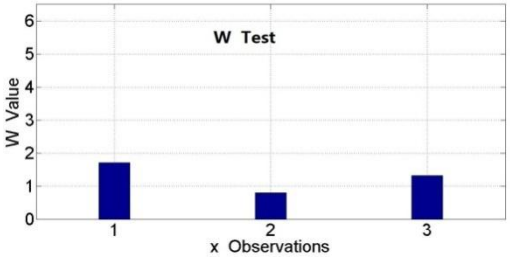

Figure 6. W-test: Data Snooping of x Image Coordinate (Point 2 with three images)

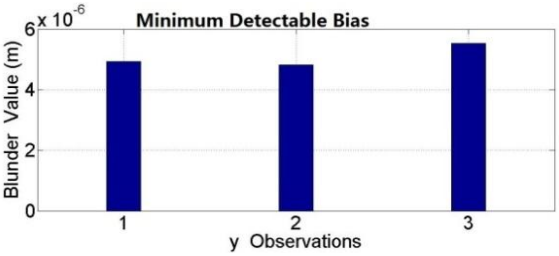

Figure 7.Minimum Detectable Bias of y Image Coordinate (Point 2 with three images)

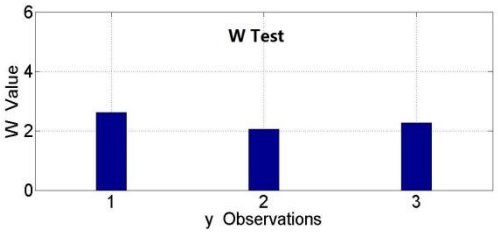

Figure 8. W-test: Data Snooping of y Image Coordinate (Point 2 with three images)

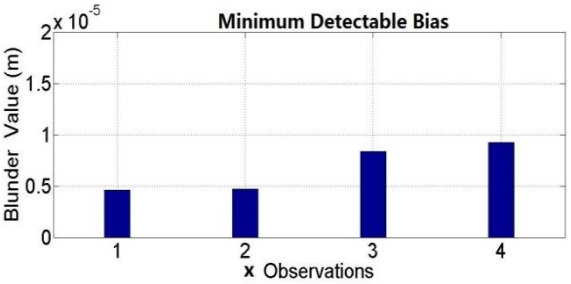

Figure 9 Minimum Detectable Bias of x Image Coordinate (Point 2 with four images)

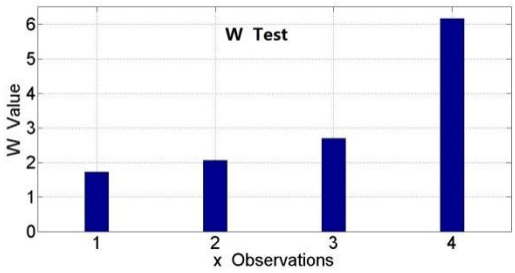

Figure10 W-test: Data Snooping of x Image Coordinate (Point 2 with four images)

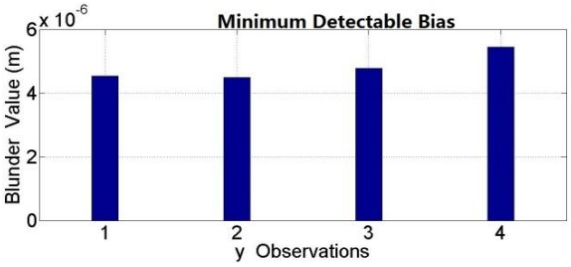

Figure 11 Minimum Detectable Bias of y Image Coordinate (Point 2 with four images)

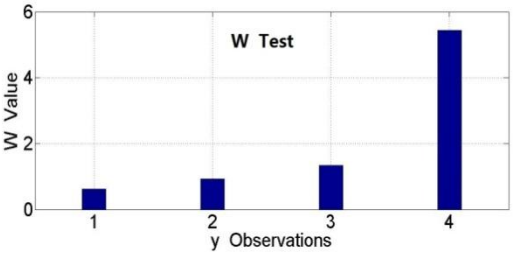

Figure12 W-test: Data Snooping of y Image Coordinate (Point 2 with four images)

mm, 138 mm, 18 mm on X, Y and Z respectively. The fourth image should be replaced by a good image or gray-based image matching combining RANdom SAmple Consensus (RANSAC) is applied to improve the accuracy of x, y coordinates with the image frame.

4. CONCLUTIONS

Machine vision and integrated multi-sensor platform implementation in 3D mapping have been extended to various applications, e.g., for street views, mining activities. The MRI 3D maps could potentially be applied for 3D

measurement of a point position, volume, local 3D model reconstruction, based on the MRI mapping database. The quality analysis is essentially important for MRI 3D maps based spatial measurements to ensure the system provides reliable products for users. According to the experiments, larger amount of overlapping images will help to improve the DOP values of object points, especially in the cases from 2 observing images to 4 observing images.

REFERENCES

Gruen, A 1985. “Adaptive least squares correlation: a powerful image matching technique”. South African Journal of Photogrammetry, Remote Sensing and Cartography, vol. 14, no. 3, pp. 175-187

.

Kavouras,M, 1982, "On the Detection of Outliers and the Determination of Reliability in Geodetic Networks", Technical Report No 87. Dept. of Surveying Engineering, Univ. of New Brunswick, Fredericton, N.B., Canada.

Lowe, D.G., 2004. “Distinctive Image Features from Scale-invariant Keypoints”. International Journal of Computer Vision, vol.60, no.2,pp.91-110.

Luhmann,T, 2009, “Precision potential of photogrammetric 6DOF pose estimation with a single camera”. ISPRS Journal of Photogrammetry and Remote Sensing, vol. 64, no. 3, pp. 275-284.

Makarovic,B. 1995, “Image-based digital mapping”. ISPRS Journal of Photogrammetry & Remote Sensing, vol. 50, no. 2, pp. 21-29.

Teunissen, P.J.G.; 1990, "Quality control in integrated navigation systems," Aerospace and Electronic Systems Magazine, IEEE , vol.5, no.7, pp.35-41, Jul

Wang J, Chen Y (1994) “On the reliability measure of observations”. Acta Geodaet et Cartograph Sin. pp 42–51 (English edition)